

AD-A116 571

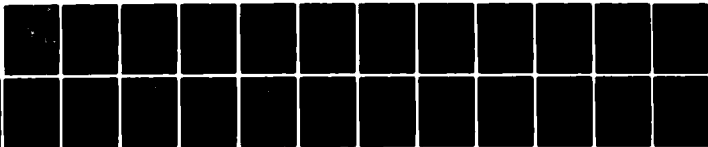
NAVAL POSTGRADUATE SCHOOL MONTEREY CA  
GENERATION RATE OF MARINE AEROSOLS AS DETERMINED FROM A BOUNDAR--ETC(U)  
MAY 82 C W FAIRALL; K L DAVIOSON  
NPS63-82-003

F/G 4/1

UNCLASSIFIED

NI

| 04 |  
AD A  
11067



END  
DATE  
FILMED:  
04-82  
DTIC

NPS63-82-003

2

# NAVAL POSTGRADUATE SCHOOL

Monterey, California

AD A116571



DTIC  
ELECTE  
JUL 7 1982  
S D D

GENERATION RATE OF MARINE AEROSOLS AS  
DETERMINED FROM A BOUNDARY LAYER MODEL

by

C. W. Fairall, K. L. Davidson,  
and G. E. Schacher

May 1982

Technical Report

Approved for public release; distribution unlimited.

Prepared for: Naval Air Systems Command  
AIR-370  
Washington, DC 20360

DTIC FILE COPY

82 07 07 078

NAVAL POSTGRADUATE SCHOOL  
Monterey, California

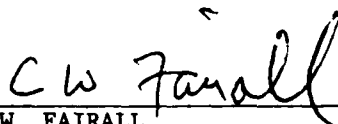
Rear Admiral J. J. Ekelund  
Superintendent

David A. Schradly  
Acting Provost

The work reported herein was supported in part by the Naval Air Systems Command, AIR-370, Washington, DC 20360.

Reproduction of all or part of this report is authorized.

This report was prepared by:

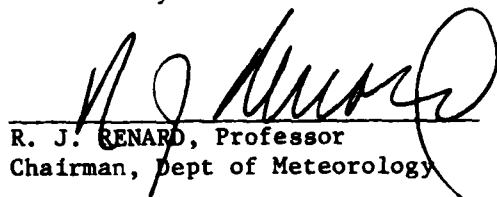


C. W. FAIRALL  
BDM Corporation Contract Employee



K. L. DAVIDSON, Professor  
Department of Meteorology

Reviewed by:

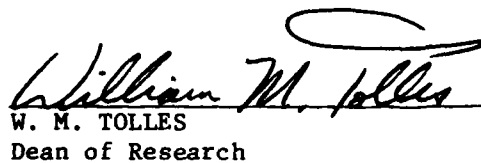


R. J. RENARD, Professor  
Chairman, Dept of Meteorology



G. E. SCHACHER, Professor  
Department of Physics

Released by:



W. M. TOLLES  
Dean of Research

Unclassified

SECURITY CLASSIFICATION OF THIS PAGE (When Data Entered)

REPORT DOCUMENTATION PAGE		READ INSTRUCTIONS BEFORE COMPLETING FORM
1. REPORT NUMBER NPS-63-82-003	2. GOVT ACCESSION NO. ADA 110511	3. RECIPIENT'S CATALOG NUMBER
4. TITLE (and Subtitle) Generation Rate of Marine Aerosols as Determined from a Boundary Layer Model		5. TYPE OF REPORT & PERIOD COVERED Technical Report 01-10-81 to 30-09-82
		6. PERFORMING ORG. REPORT NUMBER
7. AUTHOR(s) C. W. Fairall, * K. L. Davidson, G. E. Schacher		8. CONTRACT OR GRANT NUMBER(s)
9. PERFORMING ORGANIZATION NAME AND ADDRESS Naval Postgraduate School Monterey, California 93940		10. PROGRAM ELEMENT, PROJECT, TASK AREA & WORK UNIT NUMBERS 61153N; N0001982WR21036
11. CONTROLLING OFFICE NAME AND ADDRESS Naval Material Command (EO/MET) and Naval Air Systems Command (AIR 370) Washington, DC 20360		12. REPORT DATE May 1982
		13. NUMBER OF PAGES 29
14. MONITORING AGENCY NAME & ADDRESS (if different from Controlling Office)		18. SECURITY CLASS. (of this report) Unclassified
		18a. DECLASSIFICATION/DOWNGRADING SCHEDULE
16. DISTRIBUTION STATEMENT (of this Report)  Approved for public release; distribution unlimited.		
17. DISTRIBUTION STATEMENT (of the abstract entered in Block 20, if different from Report)		
18. SUPPLEMENTARY NOTES  * BDM Corporation, Contract employee		
19. KEY WORDS (Continue on reverse side if necessary and identify by block number)  Aerosols, Aerosol Modeling, Marine Aerosol Generation		
20. ABSTRACT (Continue on reverse side if necessary and identify by block number)  - The rate of generation of aerosols by bubbles bursting at the sea surface is not well known. Unfortunately, the rate is a very difficult parameter to measure. The rate can be inferred from a boundary layer model that includes determining evolutions of aerosol spectra from parameterizations of generation, transport and removal processes. Using		

DD FORM 1473  
1 JAN 73

EDITION OF 1 NOV 65 IS OBSOLETE 1  
S/N 0102-014-6601

Unclassified

SECURITY CLASSIFICATION OF THIS PAGE (When Data Entered)

Unclassified

SECURITY CLASSIFICATION OF THIS PAGE(When Data Entered)

this technique, data from CEWCOM-78 have been analyzed to produce the aerosol surface flux volume spectrum from 0.8 to 15  $\mu\text{m}$  radius at a wind speed of 9 m/sec. Using this flux spectrum and equilibrium aerosol spectra from JASIN, flux spectra are calculated for wind speeds from 6 to 18 m/sec.

TABLE OF CONTENTS

1. INTRODUCTION - - - - - 6

2. AEROSOL SPECTRUM - - - - - 8

3. FLUX SPECTRUM ANALYSIS - - - - - 12

4. FLUX SPECTRUM AND WIND SPEED - - - - - 18

5. NON-EQUILIBRIUM - - - - - 20

REFERENCES - - - - - 24

DISTRIBUTION LIST - - - - - 25

Accession For	
NTIS GRA&I	<input checked="" type="checkbox"/>
DTIC TAB	<input type="checkbox"/>
Unannounced	<input type="checkbox"/>
Justification	
By _____	
Distribution/	
Availability Codes	
Dist	Avail and/or Special
A	

DTIC  
COPY  
INSPECTED  
2

LIST OF TABLES

I. CEWCOM-78 meteorological and aerosol data for the time period analyzed for this report. The aerosol volume spectral density  $dV/dr$  is given at each radius in  $\mu\text{m}$ . The height of the boundary layer was determined from an acoustic sounder - - - - - 13

II. Equilibrium sea-salt aerosol-spectra in  $\mu\text{m}^2/\text{cm}^3$  as a function of radius ( $\mu\text{m}$ ) and wind speed (m/sec) - - - - - 19

III. Surface sea-salt aerosol flux,  $F_s(r)$ , ( $\mu\text{m}^2/\text{cm}^2/\text{sec}$ ) as a function of particle radius<sup>s</sup> ( $\mu\text{m}$ ) and wind speed (m/sec) - - - - - 19

IV. The equilibrium time constant for aerosols at  $S = 0.8$ ,  $h = 400$  m and  $W_e = 0.4$  cm/sec - - - - - 20

LIST OF FIGURES

Figure

- 1 Ensemble average total aerosol volume spectra from JASIN. The number to the right of the spectrum is the wind speed category in m/sec - - - - - 10
- 2 Time series of atmospheric  $^{222}\text{Rn}$  activity (solid line, Larsen, Kasemir and Bressan, 1979) and continental aerosol coefficient, A (dashed line) - - - - - 11
- 3 Time series of the terms of Eqn (9) for 2  $\mu\text{m}$  radius and 15  $\mu\text{m}$  radius particles. The dashed line is the average contribution of the surface production term and should be the sum of the other three terms - - - - - 15
- 4 The ensemble average surface flux spectrum,  $F_s(r)$ , for the CEMCOM-78 analysis period (average wind speed, 9 m/sec) - - - - - 16
- 5 Ensemble average contribution of entrainment ( $W_e$ ), Stokes fallout ( $W_s$ ) and surface flux  $W_F = F_s/V_s$  assuming a state of dynamic equilibrium - - - - - 17
- 6 Ensemble average equilibrium sea salt volume spectra from JASIN. The number to the right of the spectrum is the wind speed category in m/sec - - - - - 21
- 7 Ensemble average surface flux spectra deduced from Eqn (11) and Table II. The number to the right of the spectrum is the wind speed in m/sec - - - - - 22
- 8 Changes in aerosol spectral density ( $dV_s/dt$ ) versus changes in mixing volume ( $-dh/dt$ ). This graph illustrates the dominance of these terms in Eqn (9) for short time periods - - - - - 23

## 1. INTRODUCTION

This is one of a series of reports dealing with modeling of the marine atmospheric boundary layer. The basics of the Naval Postgraduate School modeling approach are given in Fairall (1981). That report also describes the current status of modeling the pertinent physical processes. The utility of the model for tactical use and initial model validation are given in Davidson et al (1982). This report is in a somewhat different vein. The other reports deal with use of the model to describe or predict the evolution of boundary layer properties. Here we use the model "in reverse" to determine an important physical parameter, the rate of generation of marine aerosols.

There are two components to aerosols in the marine boundary layer: 1) continental (background) and 2) locally generated sea-spray droplets (Barnhardt and Streete, 1970). The sea-spray droplets are generated primarily by the bursting of bubbles at the sea surface (Blanchard and Woodcock, 1957). The bubbles are produced by biological activity, chemical reaction and breaking waves (whitecaps). Thus, the sea surface is a continuous source of sea-salt aerosols in the marine boundary layer. At wind speeds greater than about 3 meters per second, whitecaps are the primary contributor to the bursting bubbles. These surface produced aerosols can be characterized by a surface flux spectrum,  $F_g(r)$ , which represents the volume of aerosol per particle radius interval produced per square centimeter of ocean surface each second as a function of aerosol particle radius. This quantity is a function of wind speed.

The continuous production of sea-salt aerosols is balanced by several removal mechanisms. One obvious mechanism is the loss of particles as they fall back to the surface. This settling under gravity is called "Stokes fall-out" and is characterized by the Stokes velocity. The particles are transported vertically by turbulence in the marine boundary layer and maintained at

a nearly uniform mixing ratio throughout the mixed layer. The growth of the height of the layer constitutes another loss mechanism called "entrainment" (Deardorff, 1976). The final loss mechanism is "rainout" which occurs when the particles become condensation nuclei in the formation of clouds.

Given the surface flux spectrum and a parameterization of the removal mechanisms, one could predict evolutions of the aerosol density spectrum (Fairall et al, 1982). Unfortunately, the surface flux spectrum is not known. However, we can reverse the process—that is, use parameterizations of the removal processes and evolutions of the aerosol spectrum—to obtain estimates of the surface flux spectrum. This paper describes the calculation of  $F_s(r)$  from data taken by the NPS Environmental Physics Group during the Cooperative Experiment for West Coast Oceanography and Meteorology (CEWCOM-78) and the Joint Air-Sea Interaction Experiment (JASIN). Details about the experiments, equipment, measurements, and analysis are given by Fairall (1981).

## 2. AEROSOL SPECTRUM

The first step to analyzing the evolution of the aerosol spectrum is to remove those variations due to changes in the ambient relative humidity. This is done by transforming each spectrum to a reference relative humidity (RH = 80% or a saturation ratio  $S = 0.8$ ). We make the usual assumption that the particle radius at saturation  $S$  is given by (Fitzgerald, 1975)

$$r_S = r \cdot g(S) \quad (1)$$

where  $r$  is the radius at  $S = 0.8$  and  $g(S) = 0.81 \exp [0.066S/(1.058-S)]$ . If we have a measured aerosol number density spectrum,  $n'(r_S)$ , then the transformed spectrum at standard saturation,  $n(r)$ , is:

$$dn/dr = n(r) = n'(r \cdot g(S)) \cdot g(S) \quad (2)$$

Since we prefer to work with the volume spectrum  $V(r) = 4/3\pi r^3 n(r)$ , the corresponding relationship is:

$$dV/dr = V(r) = V'(r \cdot g(S)) / g^2(S) \quad (3)$$

We now must separate the measured spectrum into its two basic components:

- 1) The background continental aerosol of nonlocal origin,  $V_C$ , which is present above and within the marine layer; and
- 2) The sea-salt aerosol locally generated at the sea surface,  $V_S$ , which is well mixed throughout the marine layer ( $h$  is the height of the mixed layer). Thus, we assume:

$$V(r) = V_C(r) + V_S(r) \quad Z < h \quad (4a)$$

$$V(r) = V_C(r) \quad Z > h \quad (4b)$$

The continental aerosol component is represented with a Junge type distribution,

$$V_C(r) = A/r \quad (5)$$

where  $A$  is the continental coefficient. Since there is very little sea-salt volume production for  $r < 0.3 \mu\text{m}$ , we can use the small size range of the

spectrum to calculate the continental coefficient ( $A = rV(r)$ ). This is documented in Fig. 1 where ensemble averages of volume spectra indicated that  $V(r)$  is essentially independent of wind speed at  $r = 0.1 \mu\text{m}$ . At low wind speeds, the  $r = 0.1 \mu\text{m}$  and  $r = 0.3 \mu\text{m}$  ensemble average spectra are described quite accurately by Eqn (5). The claim that  $A$  is an accurate index of continental influence is nicely validated by comparison with atmospheric Radon activity (Larsen et al, 1979) from CEWCOM-78 (Fig. 2). Thus, the locally generated sea-salt component can be calculated using:

$$V_s(r) = V(r) - A/r \quad (6)$$

The remainder of this report will deal exclusively with the volume spectra transformed to standard humidity,  $V_s(r)$ . We write this as  $V_s$  to simplify the notation--with the understanding that  $V_s$  refers to the spectrum at RH = 80%, with radius,  $r$ , an implied variable.

The evolution of the aerosol spectrum in the well mixed marine boundary is described by the following equation (Fairall et al, 1982),

$$h dV_s/dt = F_s - (W_e + W_s) V_s \quad (7)$$

(which is presented here without further discussion)

where  $W_e$  is the entrainment velocity and  $W_s$  is the Stokes velocity (Wu, 1979)

$$W_s = 1.57 \times 10^{-2} (1 + 1.2(0.81/g(S))^3) r^2 g^2(S) \quad (8a)$$

$$W_e = dh/dt - \bar{w} \quad (8b)$$

where  $r$  is in  $\mu\text{m}$ ,  $W_s$  is in  $\text{cm/sec}$  and  $\bar{w}$  is the mean vertical air motion due to synoptic scale weather (subsidence). In Eqn (7) we have left out the cloud formation removal mechanism because it acts on a much longer time scale. One assumption implicit in Eqn (7) is that the convective mixing velocity,  $W_*$  (Kaimal et al, 1976), is much larger than  $W_s$ . Since  $W_*$  is typically 1 m/sec while  $W_s$  is on the order of 0.1 m/sec for the largest particles ( $r = 15 \mu\text{m}$ ) considered here, the assumption is reasonable.

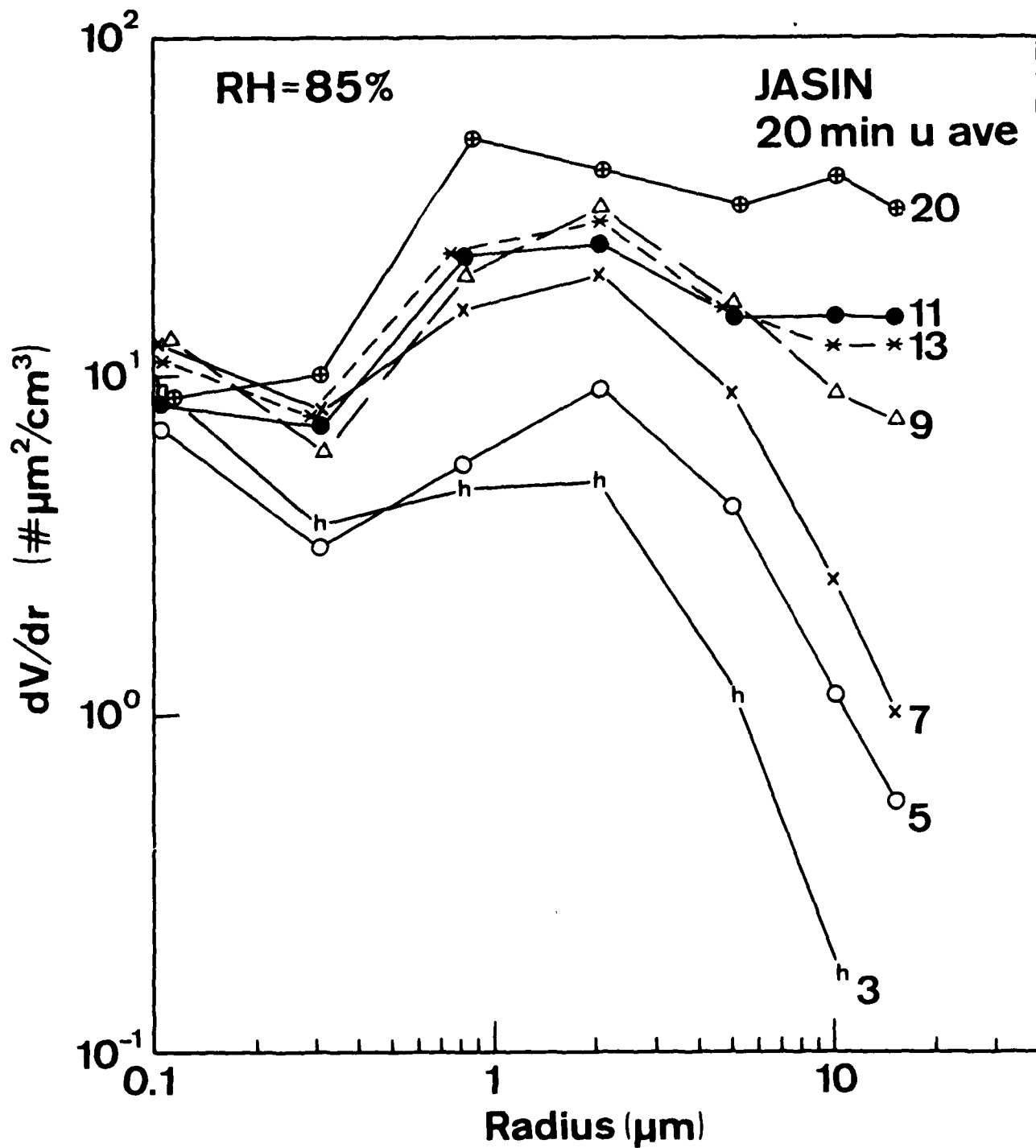


Figure 1. Ensemble average total aerosol volume spectra from JASIN. The number to the right of the spectrum is the wind speed category in m/sec.

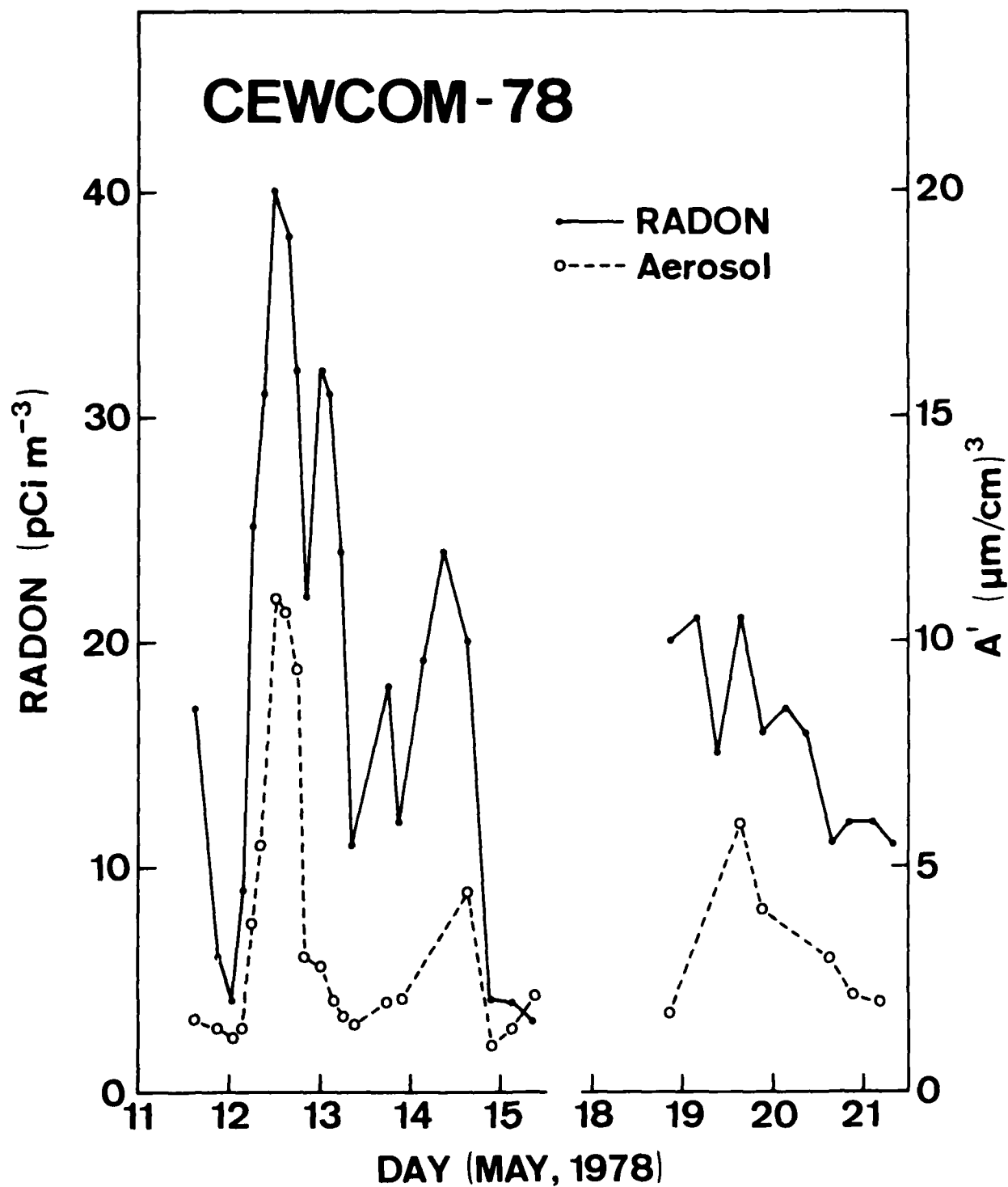


Figure 2. Time series of atmospheric <sup>222</sup>Rn activity (solid line, Larsen, Kasemir and Bressan, 1979) and continental aerosol coefficient, A (dashed line).

### 3. FLUX SPECTRUM ANALYSIS

The CEWCOM-78 data have been used to evaluate the surface flux term of Eqn (7). Since the other terms of the expression were measured, one simply calculates  $F_s$  using a rearrangement of the terms. Thus the final expression for the flux calculation is,

$$F_s = h dV_s/dt + (W_e + W_s)V_s \quad (9)$$

A period was chosen from CEWCOM-78 where all data were available, the synoptic conditions were fairly stable, the wind speed was reasonably constant and a good mixed layer was present (Table I). There was a slowly decreasing continental influence indicated by steady NW winds (A in Table I and Fig. 2).

Application of Eqn (9) requires a value for the entrainment velocity. If the subsidence velocity is known, then  $W_e$  can be calculated from  $dh/dt$  using Eqn (8b). Since it is difficult to obtain  $\bar{W}$  to 0.1 cm/s accuracy, it was decided to estimate  $W_e$  empirically from the evolution of the mixed-layer temperature and water vapor density. This was accomplished by simulating the analysis period with a dynamic mixed-layer model. After initializing the model with the atmospheric parameters at the beginning of the period, the entrainment velocity was adjusted to yield best agreement with the temperature and water vapor density at the end of the period. The mean  $W_e$  for the period was 0.35 cm/s. This implies  $\bar{W} = -0.3$  cm/s for the first 8 hours and  $\bar{W} = 0$  for the last 12 hours.

The scatter and uncertainty of the aerosol and mixed layer depth measurements introduces certain trade-offs between averaging times and statistical validity. For short averaging times, the random scatter of the individual terms is considerable, leading to large variations in the time derivative terms. By increasing the averaging time to 4 hours, the  $F_s$  "signal-to-noise" becomes more reasonable. A time series of the individual terms of Eqn (9) is

TABLE I. CEWCOM-78 meteorological and aerosol data for the time period analyzed for this report. The aerosol volume spectra density  $dV/dr$  is given at each radius  $r$ , in  $\mu\text{m}$ . The height of the boundary layer was determined from an acoustic sounder.

DATE	TIME	U (m/s)	RH (%)	h (m)	A	r=.3	r=.8	r=2 ( $\mu\text{m}^2/\text{cm}^3$ )	r=5	r=10	r=15
5/20	1130	7.4	89.4	420	7.8	15.1	12.5	9.79	2.26	0.801	0.437
5/20	1230	7.7	87.6	430	5.2	9.15	12.5	11.9	2.08	0.644	0.327
5/20	1330	8.2	86.4	430	4.5	8.39	11.9	12.2	2.91	1.11	0.628
5/20	1430	8.1	82.1	415	4.7	8.54	10.6	11.4	2.24	0.780	0.420
5/20	1530	8.3	80.9	437	4.0	7.96	12.0	11.2	1.26	0.296	0.127
5/20	1630	8.2	81.1	437	4.0	7.85	11.9	13.6	2.47	0.795	0.411
5/20	1730	9.0	82.5	443	3.6	7.26	12.9	13.4	2.55	0.854	0.455
5/20	1830	10.0	83.8	430	2.6	6.54	14.0	13.2	3.30	1.37	0.819
5/20	1930	10.3	84.3	420	2.4	6.07	13.8	13.2	3.71	1.73	1.11
5/20	2030	9.8	86.8	360	2.1	6.54	15.9	14.2	4.02	1.63	0.958
5/20	2130	10.1	87.7	377	1.9	6.07	14.9	13.2	3.34	1.22	0.678
5/20	2230	9.5	87.6	397	2.7	6.82	13.6	12.8	3.52	1.42	0.833
5/20	2330	9.2	87.6	400	2.7	6.15	12.9	12.7	3.46	1.46	0.891
5/21	30	9.6	87.3	420	3.0	6.14	13.1	11.8	2.58	0.993	0.569
5/21	130	9.2	88.3	490	2.0	5.69	13.5	12.9	3.33	1.26	0.710
5/21	230	8.3	87.4	520	1.7	5.29	13.3	13.4	3.44	1.39	0.818
5/21	330	8.2	86.1	560	2.7	6.11	11.8	10.9	2.18	0.731	0.390
5/21	430	8.5	83.1	597	2.2	5.55	11.6	9.71	1.78	0.659	0.369
5/21	530	8.2	81.3	620	2.0	5.33	10.9	9.75	1.85	0.732	0.431
5/21	630	7.9	79.7	680	1.8	5.01	11.1	10.7	1.96	0.678	0.365

shown in Fig. 3 for two different particle sizes. The average surface production flux spectrum is shown in Fig. 4. This flux spectrum applies to the average surface conditions for the entire 20 hour period (average wind speed was about 9 m/sec). The error bars represent the uncertainty in the mean estimate.

The relative contributions of entrainment, gravitational fallout and surface production are nicely illustrated by defining an equivalent surface production vertical velocity,  $W_F = F_s/V_s$  so that in equilibrium ( $dV_s/dt = 0$ )

$$W_F = W_e + W_s \quad (10)$$

For the average conditions found in the analysis period, the entrainment and Stokes terms were roughly equal at a particle radius of 5  $\mu\text{m}$  (Fig. 5).

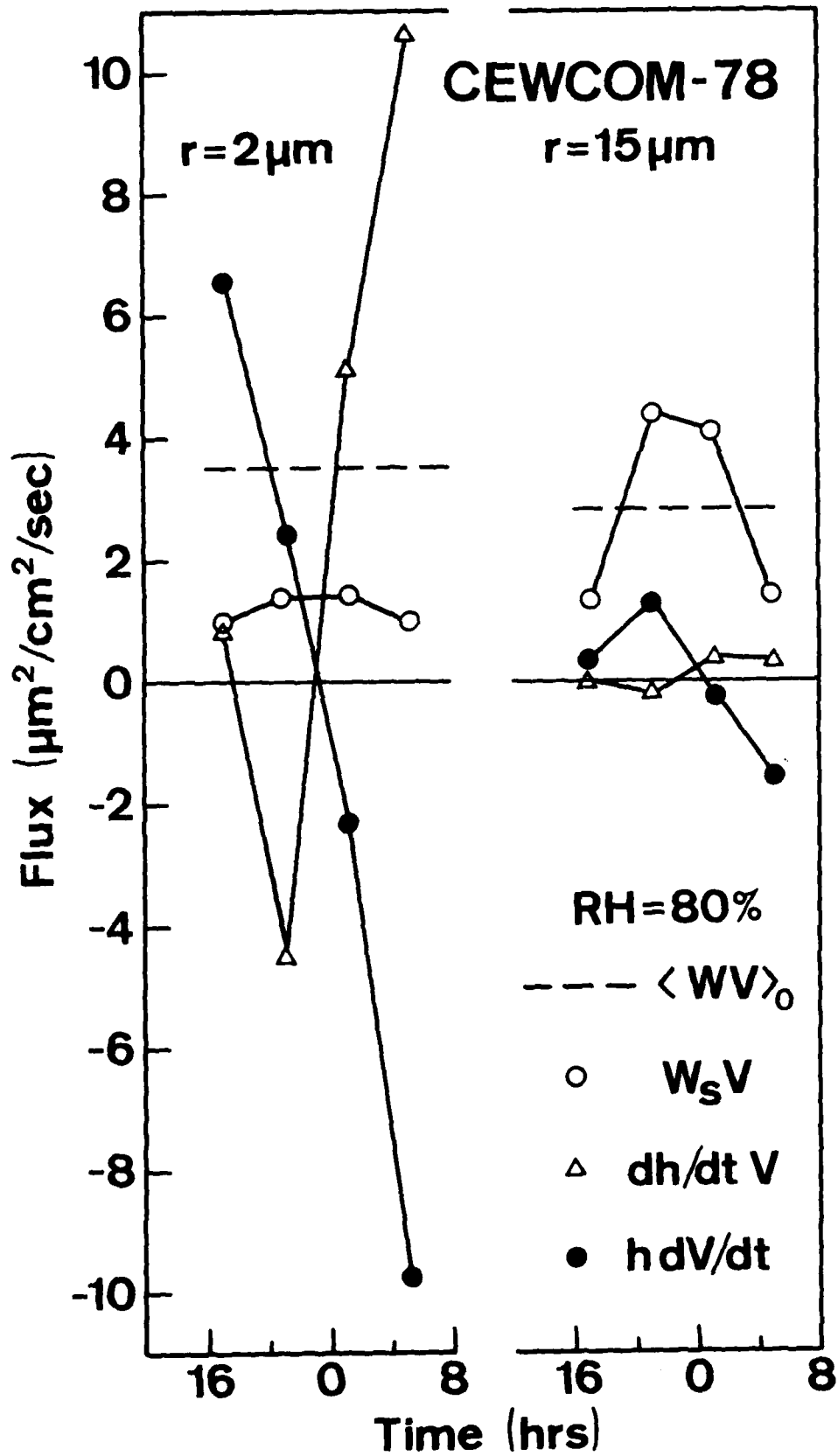


Figure 3. Time series of the terms of Eqn (9) for 2  $\mu\text{m}$  radius and 15  $\mu\text{m}$  radius particles. The dashed line is the average contribution of the surface production term and should be the sum of the other three terms.

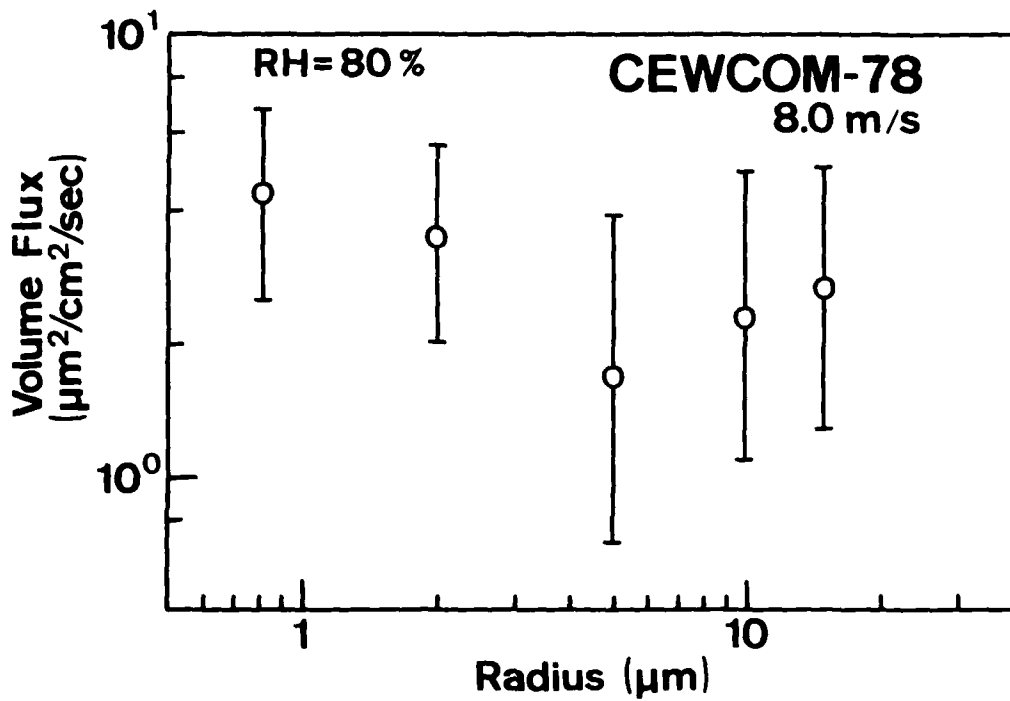


Figure 4. The ensemble average surface flux spectrum,  $F(r)$ , for the CEWCOM-78 analysis period (average wind speed, 9 m/sec).

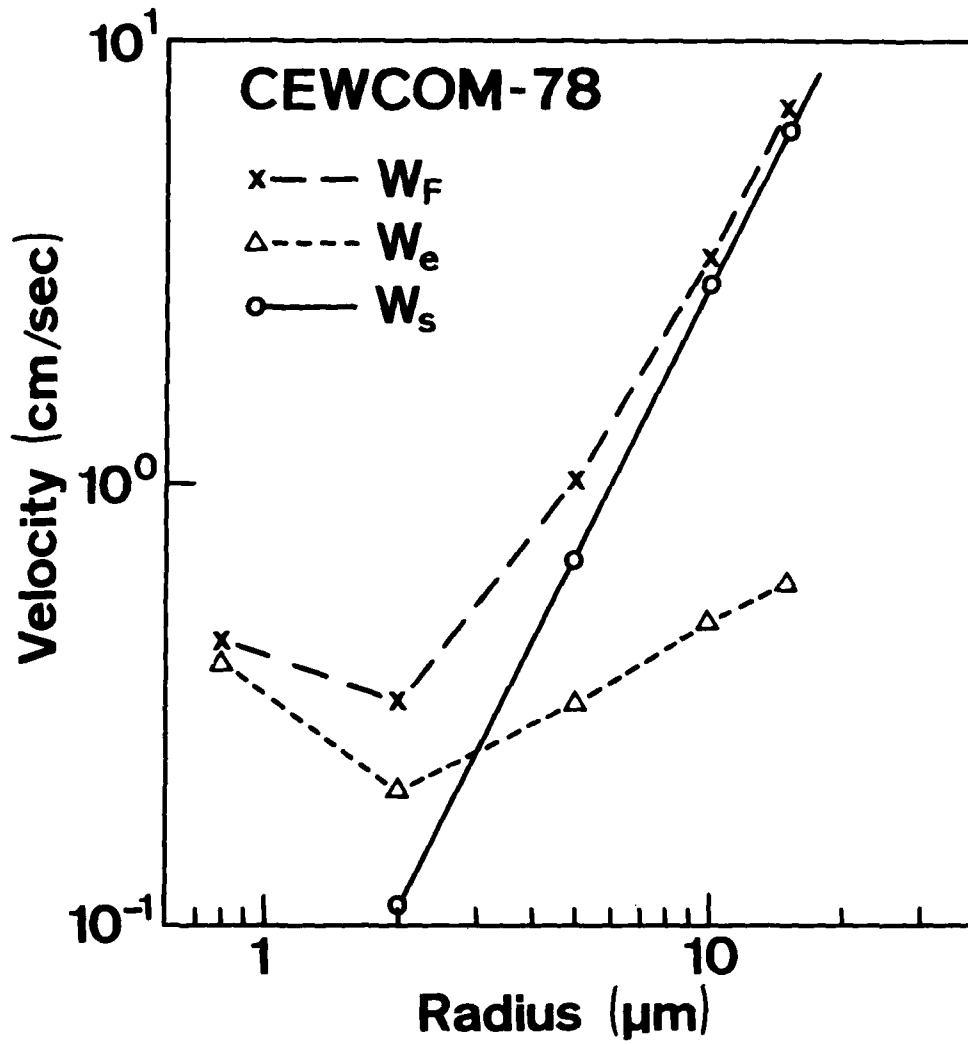


Figure 5. Ensemble average contribution of entrainment ( $W_e$ ), Stokes fallout ( $W_s$ ) and surface flux  $W_F = F_s/V_s$  assuming a state of dynamic equilibrium.

#### 4. FLUX SPECTRUM AND WIND SPEED

Because of the reasonably constant wind speeds during the 20 hour CEWCOM-78 period, we were able to improve the statistical certainty for the  $F_s$  calculation by combining all the data from the period, assuming that the flux would be a reasonable representation for  $U = .9$  m/sec wind speed. Thus, we now have the surface flux spectrum at a single wind speed. In order to estimate the flux at other wind speeds, we note that the right hand side of Eqn (10) is nearly independent of wind speed for equilibrium conditions. Therefore, the flux at one wind speed can be related to the flux at other wind speeds if the equilibrium volume spectra are known:

$$F_s(U_1) = F_s(U_2) V_s(U_1)/V_s(U_2) \quad (11)$$

We have available from JASIN a large set of ensemble averages of aerosol volume spectra at different wind speeds (Fig. 6 and Table II). It is a simple matter to apply this data to Eqn (11) using the CEWCOM-78 aerosol flux and equilibrium spectrum to generate the surface volume flux spectra as a function of wind speed (Fig. 7 and Table III). At a wind speed of 6.0 m/sec, the flux can be integrated in radius space to yield a total sea-salt dry mass production rate of  $4.8 \text{ mg/m}^2/\text{day}$  which compares well with the  $4.4 \text{ mg/m}^2/\text{day}$  estimated by Blanchard (1963) and  $4.2 \text{ mg/m}^2/\text{day}$  estimated by Kritz and Rancher (1980).

TABLE II. Equilibrium sea-salt aerosol spectra in  $\mu\text{m}^2/\text{cm}^3$  as a function of radius ( $\mu\text{m}$ ) and wind speed (m/sec).

$\downarrow$ u	r $\rightarrow$	0.8	2	5	10	15
6		2.8	3.4	3	0.3	0.05
9		10	10	5	1	0.35
11		18	25	13	6.4	4.2
13		20	30	20	15	15
15		24	33	22	22	22
18		28	35	28	28	28
9*		9	11	2	0.8	0.4

TABLE III. Surface sea-salt aerosol flux,  $F_s(r)$ , ( $\mu\text{m}^2/\text{cm}^2/\text{sec}$ ) as a function of particle radius ( $\mu\text{m}$ ) and wind speed (m/sec).

$\downarrow$ u	r $\rightarrow$	0.8	2	5	10	15
6		1.3	1.1	2.5	1.0	0.33
9		4.5	3.1	4.2	3.3	2.3
11		8.2	7.7	11	21	27
13		9.1	9.2	17	49	48
15		11	10	19	72	140
18		17	11	24	92	180
9*		4.1	3.4	1.7	2.3	2.6

\* CEWCCM-78 Analysis Period

## 5. NON-EQUILIBRIUM

For time periods of a few hours, the aerosol spectrum may not be in a state of dynamic equilibrium. If we rewrite Eqn (7) in the following form:

$$dV_s/dt + V_s/\tau_p = F_s/h$$

where the time constant,  $\tau_p$ , is

$$\tau_p = h/(W_e + W_s) \quad (13)$$

then we see the analogy of aerosols and a capacitor charged by an applied "voltage",  $F_s$ , through a "resistance",  $(W_e + W_s)^{-1}$ . In this analogy, the "capacitance" is  $h$ .

The response time of the aerosol density is a strong function of particle radius because  $W_s \sim r^2$ . Values of  $\tau_p$  for  $S = 0.8$  and  $h = 400$  m are given in Table IV.

TABLE IV. The equilibrium time constant for aerosols at  $S = 0.8$ ,  $h = 400$  and  $W_e = 0.4$  cm/sec.

$r, \mu\text{m}$	0.5	1	5	10	15
$\tau_p$ , hours	28	22	11	3.5	0.5

The boundary layer mixing time,  $\tau_m$ , which represents the time required for changes in aerosol density to be evenly distributed throughout the marine layer is:

$$\tau_m = h/W_* \quad (14)$$

For the CENCOM-78 analysis period ( $h = 400$  m and  $W_* = 0.6$  m/sec) we find  $\tau_m = 0.16$  hours. Therefore, short term variations in mixing volume ( $dh/dt$ ) will lead to changes in the aerosol density because the production response time is much slower than the mixing time. Thus, for time periods on the order of one hour, changes in the aerosol density ( $h dV_s/dt$ ) will be highly correlated with the mixing volume term ( $V_s dh/dt$ ). This effect, which is particularly noticeable for smaller particles (see Fig. 3 and Table III), is shown in Fig. 8.

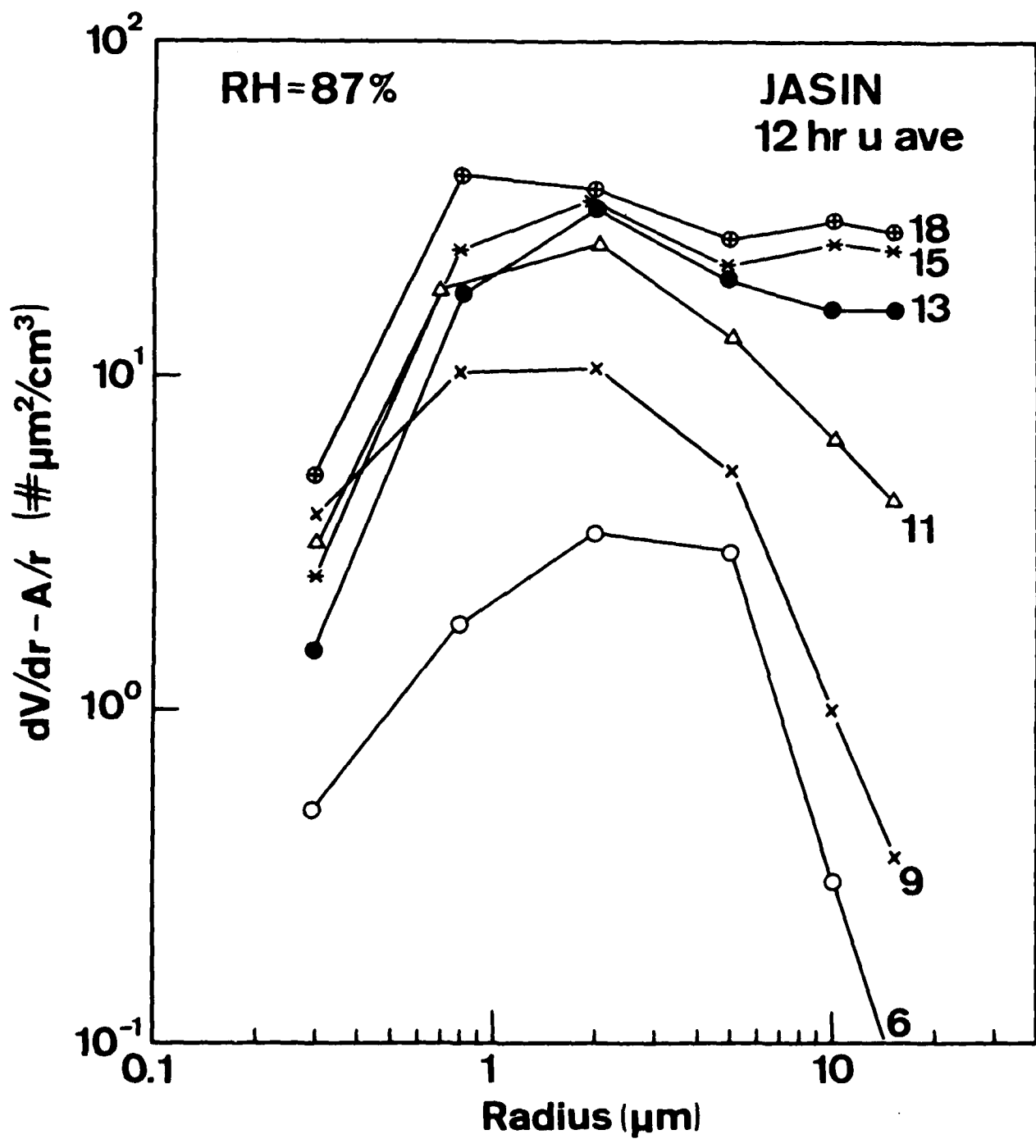


Figure 6. Ensemble average equilibrium sea salt volume spectra from JASIN. The number to the right of the spectrum is the wind speed category in m/sec.

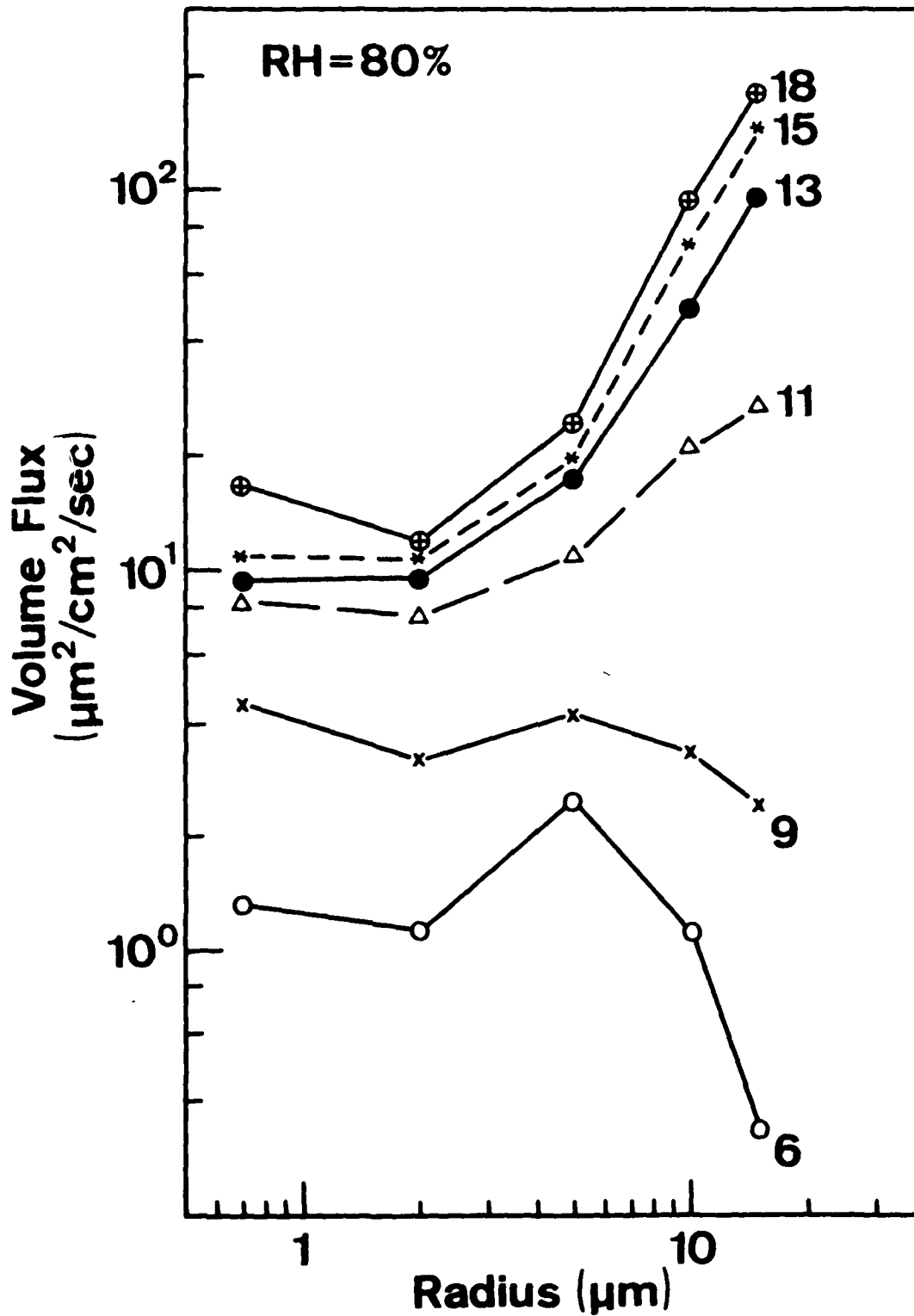


Figure 7. Ensemble average surface flux spectra deduced from Eqn (11) and Table II. The number to the right of the spectrum is the wind speed in m/sec.

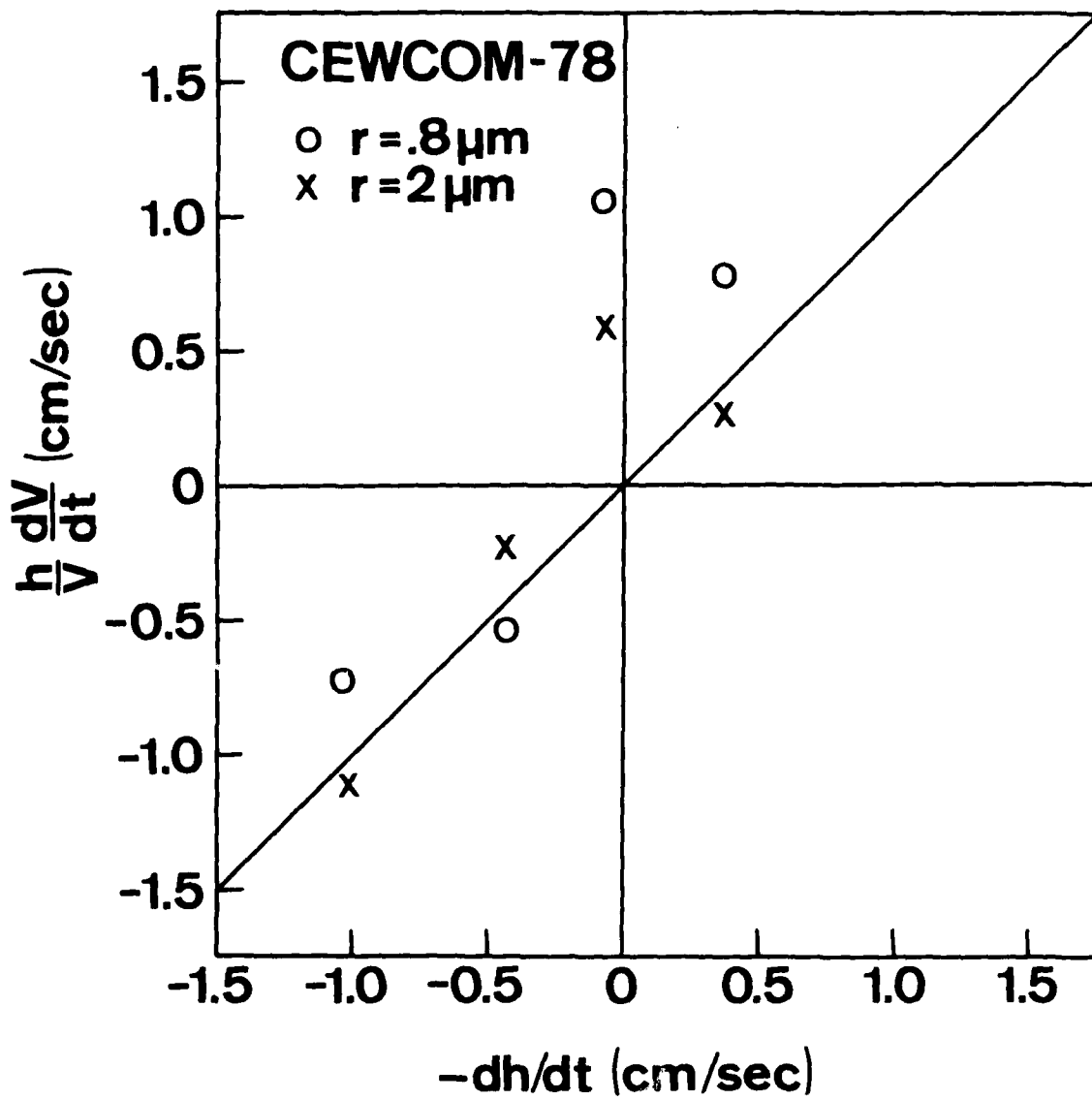


Figure 8. Changes in aerosol spectral density ( $dV/dt$ ) versus changes in mixing volume ( $-dh/dt$ ). This graph illustrates the dominance of these terms in Eqn (9) for short time periods.

## REFERENCES

- Barnhardt, E. A. and Streete, J. L., 1970. A method for predicting atmospheric aerosol scattering coefficients in the infrared. Appl. Opt., 9, 1337-1344.
- Blanchard, D. C. and Woodcock, A. U., 1957. Bubble formation and modification in the sea and its meteorological significance. Tellus, 9, 145-157.
- Blanchard, D. C., 1963. Electrification of the atmosphere by particles from bubbles in the sea. Progr. Oceanogr., 1, 71-202.
- Davidson, K. L., G. E. Schacher, C. W. Fairall, P. Boyle and D. Brower, 1982: Marine atmospheric boundary layer modeling for tactical use, Technical Report NPS63-82-001.
- Deardorff, J. W., 1976. On the entrainment rate of a stratocumulus-topped mixed layer. Quart. J. R. Met. Soc., 102, 563-582.
- Fairall, C. W., Davidson, K. L., and Schacher, G. E., 1982. Application of a mixed layer model to aerosols in the coastal marine boundary layer. Proc. First Int. Conf. on Meteorology and Air/Sea Interaction in the Coastal Zone, AMS, Boston.
- Fairall, C. W., 1981. Aerosol extinction over the ocean: a field evaluation of the Wells-Munn-Katz model. BDM Corporation, Monterey, CA, Technical Report BDM/M-Tr-001-81.
- Fitzgerald, J. W., 1975. Approximation formulas for the equilibrium size of an aerosol particle as a function of its dry size and composition and the ambient relative humidity. J. Appl. Meteor., 14, 1044-1049.
- Kritz, M. A. and Rancher, J., 1980. Circulation of Na, Cl, and Br in the tropical marine atmosphere. J. Geophys. Res., 85, 1633-1639.
- Larsen, R. E., Kasimir, W. and Bressan, D. J., 1979. Measurements of atmospheric <sup>222</sup>Rn at San Nicolas Island and over nearby California coastal areas during CEWCOM-78. Naval Research Laboratory, Washington, DC, Technical Report 3941.
- Wu, J., 1979. Spray in the atmospheric surface layer: review and analysis of laboratory and oceanic results. J. Geophys. Res., 84, 1693-1704.

DISTRIBUTION LIST

	No. of Copies
1. Defense Technical Information Center Cameron Station Alexandria, Virginia 22314	2
2. Library, Code 0142 Naval Postgraduate School Monterey, California 93940	2
3. Dean of Research, Code 012 Naval Postgraduate School Monterey, California 93940	1
4. Professor J. Dyer, Code 61Dy Naval Postgraduate School Monterey, California 93940	1
5. Professor R. J. Renard, Code 63Rd Naval Postgraduate School Monterey, California 93940	1
6. Professor C.N.K. Mooers, Code 68Mr Naval Postgraduate School Monterey, California 93940	1
7. Professor K. L. Davidson, Code 63Ds Naval Postgraduate School Monterey, California 93940	10
8. Professor G. E. Schacher, Code 61Sq Naval Postgraduate School Monterey, California 93940	10
9. Asst Prof R. W. Garwood, Code 68Gd Naval Postgraduate School Monterey, California 93940	1
10. Dr. C. W. Fairall BDM Corporation 1340 Munras Street Monterey, California 93940	10
11. Mr. Don Spiel BDM Corporation 1340 Munras Street Monterey, California 93940	2
12. Dr. A. Weinstein Director of Research Naval Environmental Prediction Research Facility Monterey, California 93940	1

13. CAPT K. Van Sickle 1  
Naval Environmental Prediction Research Facility  
Monterey, California 93940
14. Dr. A. Gorooh 1  
Naval Environmental Prediction Research Facility  
Monterey, California 93940
15. Dr. Paul Twitchell, Code 370C 1  
Naval Air Systems Command  
Washington, DC 20360
16. Dr. Alex Shlanta, Code 3173 1  
Naval Weapons Center  
China Lake, California 93555
17. Dr. Barry Katz, Code R42 1  
Naval Surface Weapons Center  
White Oak Laboratory  
Silver Spring, Maryland 20362
18. Dr. J. H. Richter, Code 532 1  
Naval Ocean Systems Center  
San Diego, California 92152
19. Dr. Lothar Ruhnke, Code 8320 1  
Naval Research Laboratory  
Washington, D.C. 20375
20. Mr. Herb Hitney, Code 532 1  
Naval Ocean Systems Center  
San Diego, California 92152
21. Mr. Herb Hughes, Code 532 1  
Naval Ocean Systems Center  
San Diego, California 92152
22. Mr. Stuart Gatham, Code 8320 1  
Naval Research Laboratory  
Washington, DC 20375
23. Commander, RMS-405 1  
Naval Sea Systems Command  
Washington, DC 20360
24. Dr. Steven Burke 1  
Naval Environmental Prediction Research Facility  
Monterey, California 93940
25. Mr. Sam Brand 1  
Naval Environmental Prediction Research Facility  
Monterey, California 93940

26. Mr. Paul Banas, Code 9220 1  
 Naval Oceanographic Office  
 NSTL Station, Mississippi 39522
27. Dr. Paul Moersdorf, Code 9220 1  
 Naval Oceanographic Office  
 NSTL Station, Mississippi 39522
28. LT Mark Schultz 1  
 Naval Environmental Prediction Research Facility  
 Monterey, California 93940
29. Mr. Ted Zuba, Code AIR-370 1  
 Naval Air Systems Command  
 Washington, DC 20360
30. Mr. Jay Rosenthal 1  
 Geophysics Division  
 Pacific Missile Range  
 Point Mugu, California 93042
31. Dr. Michael J. Kraus 1  
 AFGL/LYS  
 Hanscom AFB, Massachusetts 01731
32. MAJ Bob Wright 1  
 AWS/DOOE  
 Scott AFB, Illinois 62225
33. MAJ Ed Kolczynski 1  
 AWS/SYX  
 Scott AFB, Illinois 62225
34. Joel S. Davis 1  
 Defense Sciences Division  
 Science Applications, Inc.  
 1010 Woodman Drive, Suite 200  
 Dayton, Ohio 45432
35. Mr. L. Biberman 1  
 Institute for Defense Analysis  
 400 Army Navy Drive  
 Arlington, Virginia 22202
36. Dr. Richard Gomez 1  
 DELAS-EO-MO  
 Atmospheric Sciences Laboratory  
 White Sands, New Mexico 88002
37. Dr. R. Fenn 1  
 Air Force Geophysics Laboratory  
 Hanscom AFB, Massachusetts 02173

- 38. Mr. Glen Spaulding, MAT 72 1  
 Naval Material Command  
 Washington, DC 20362
  
- 39. CDR Thomas Callahan, Code N341 1  
 Naval Oceanography Command  
 NSTL Station, Mississippi 39529
  
- 40. CAPT Ronald Hughes, Commander 1  
 Naval Oceanography Command  
 NSTL Station, Mississippi 39529
  
- 41. CAPT Ernie Young, OP 952 1  
 Oceanographer of the Navy  
 Washington, DC 20360
  
- 42. Dr. Lowell Wilkens 1  
 Naval Weapons Center  
 China Lake, California 93553
  
- 43. Dr. Ed Monahan 1  
 Department of Oceanography  
 University College  
 Galway, IRELAND
  
- 44. Mr. Walter Martin, Code 470 1  
 Office of Naval Research  
 800 N. Quincy Street, Rm 307  
 Arlington, Virginia 22217
  
- 45. Dr. Gloria Patton 1  
 Office of Naval Research  
 1030 E. Green Street  
 Pasadena, California 91106
  
- 46. Mr. Jim Hughes, Code 470 1  
 Office of Naval Research  
 800 N. Quincy Street  
 Arlington, Virginia 22217
  
- 47. Dr. Warren Denner 1  
 Science Applications, Inc.  
 2999 Monterey-Salinas Hwy  
 Monterey, California 93940
  
- 48. Mr. George Hanssen 1  
 Science Applications, Inc.  
 P.O. Box 1303  
 1710 Goodrich Drive  
 McLean, Virginia 22102

49. Dr. Lou Goodman, Code 481 1  
Office of Naval Research  
Physical Oceanography  
NSTL Station, Mississippi 39529
50. CDR S. G. Colgan, Code 420B 1  
Office of Naval Research  
800 N. Quincy Street  
Arlington, Virginia 22217
51. Dr. John A. Cooney 1  
Dept of Physics and Atmospheric Science  
Drexel University  
Philadelphia, Pennsylvania 19104
52. Mr. Thomas Rappolt 1  
Energy Resources Company, Inc.  
3344 N. Torrey Pines Court  
La Jolla, California 92037
53. MAJ Gary G. Worley 1  
Air Force Engineering and Services Center  
Tyndall AFB, Florida 32403

FILMED

8-8